Using the Virtual Resistance Control Method to Reduction Oscillations in the Input LC Filter of AC-DC Rectifiers

MOHAMMAD ALI SHAMSI NEJAD[1,*] **AND ABBAS MOHAMMADI**[1]

[1] *Department of Electrical and Computer Engineering, University of Birjand, Avini Blvd., Birjand, Iran.*

Manuscript received 14 May, 2022; revised 13 October, 2022; accepted 17 October, 2022. Paper no. JEMT-2205-1385.

This paper examines an important topic called Total Harmonic Distortion (THD) of input current in ac-dc rectifiers. It is especially important in high-power electric vehicle charging stations, which causes oscillations in the power grid.Since the in the rectifiers the input LC filter has the role of filtering and reducing oscillations.In this paper, changes are applied to the rectifier controller, which makes the LC filter behave like an RLC filter.which causes the damping of the input current oscillations to the power grid. Since it does not use any real resistance, the efficiency of the converter does not decrease and losses do not increase. Therefore, it is called virtual resistance control method. It can be considered in series or parallel with inductor or capacitor.This research is to reduce oscillations in high power loads in steady state, which can reduce losses in the filters of the chargers. In the following, the simulation results of the battery charger rectifier are in steady state, And finally to validate it The proposed method has been implemented in a laboratory and the results have been displayed. © 2023 Journal of Energy Management and Technology

keywords: *battery charger, electric vehicle, converter, rectifier, virtual resistance*

http://dx.doi.org/10.22109/JEMT.2022.342345.1385

NOMENCLATURE

EVs	electric vehicles.
$F-bridge$	Full bridge.
$G2V$	Grid-to-Vehicle.
I_{in}	the input current of rectifier.
I_{ac}	the current of the network input.
${i_{in}}^*$	the input reference current of the charger.
PWM	pulse width modulation.
$R_{1,2,3,4}$	the virtual resistance.
THD	the total harmonic distortion.
V_{ac}	the voltage of the network input.
V_{dc}	the DC-link voltage.

1. INTRODUCTION

Figure 1 shows the voltage type of PWM AC-DC converter circuits. An input LC filter is commonly used in AC-DC PWM converters to minimize input current harmonics. Because the resistance of the LC filter is usually very low, the oscillation is damped slowly and continuous fluctuations are observed in the resonant frequency of the LC filter. Under these conditions, the source flow will be severely disturbed [1, 2]. Various methods have been proposed for damping oscillations in the input LC filter. These methods require additional current and voltage sensors and are designed and usually difficult to design. In this paper, a new control method for fluctuation damping in the input LC filter of AC-DC PWM converters is proposed. Fluctuations in the input LC filter are neutralized using a virtual resistor. A virtual resistor is an additional control algorithm that causes the LC filter to behave as if a real resistor were connected. Since no real resistance is used, the oscillations can be neutralized without compromising performance. The implementation of the virtual resistor depends on how the resistor is connected to the LC filter. The resistor can be connected in series or in parallel to the inductor or filter capacitor. Four possible connections of virtual resistors are described in this paper. The results show that fluctuations in the input LC filter can be effectively neutralized using the provided virtual resistor [3, 4]. Here, a new control method has been implemented in the laboratory to prove the correct operation. Due to the lack of features and only to show the performance of the new controller, an acidic battery has been used for the charger output. And laboratory results show that the harmonic input current is reduced. And this method can be used in high power chargers as well as in the vehicle [5]. By reviewing various papers, the approach of several

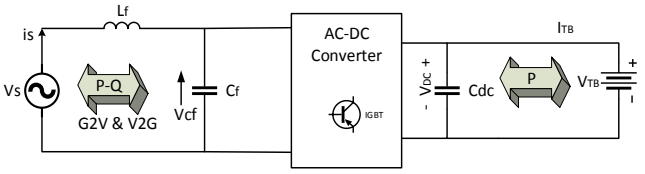

Fig. 1. Single-phase rectifier diagram.

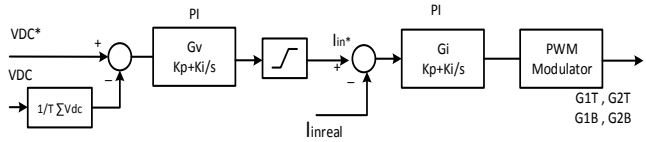

Fig. 2. Rectifier control block.

papers on the topic of virtual resistance is given. It is stated in the paper [6] In order to achieve equilibrium stability, a virtual resistor is added as a damping factor in power shaping passivity based controller. The controller is based on energy modification in which its control of energy is done through suitable damping injection by incorporating a virtual resistor in series with the inductor or in parallel to the capacitor. It is stated in the paper [7], A virtual-resistor-based active damping approach is presented and analyzed to modify the output impedance of the rectifier and improve the stability of the system under all operating modes irrespective of the power flow direction. It is stated in the paper [8], This control method is to deliver a stable operation of dc charger voltage at the specified range and produces good power quality on both input and output.

2. AC-DC CONVERTER

Figure 1 shows a diagram of a PWM AC-DC voltage inverter with an LC filter on the input side. This converter is usually controlled using a dual loop controller. The outer loop controls the DC output voltage and the inner loop controls the input current of the converter.

Various PWM techniques for controlling the converter input current have been proposed in the literature. As shown in Figure 2 of the control block diagram in the inner loop, the actual DC output voltage is initially compared to a voltage reference, which is to receive the DC output voltage error signal. The error signal is then processed by the DC output voltage controller to determine the reference of the converter input current (the controller is usually used here (PI)). In the outer loop, the converter input current reference is compared to the actual current value to determine the input error signal. The error signal is then processed by the converter input current controller and applied to the rectifier converter through the PWM switching pattern [7]. The LC filter is usually designed to have a resonant frequency lower than the lowest harmonic frequency. If the converter is controlled using the PWM technique, which has a constant switching frequency, the design is relatively simple because we can only select the resonant frequency, which is less than the switching frequency. If the converter is controlled using a variable frequency hysteresis controller, it is difficult to determine the lowest harmonic frequency. There is a possibility that the lowest harmonic frequency is equal to the resonant frequency of the LC filter. If the resonant frequency is designed to be very low, the filter size will be very large. To reduce losses in the filter, the noise resistance of the

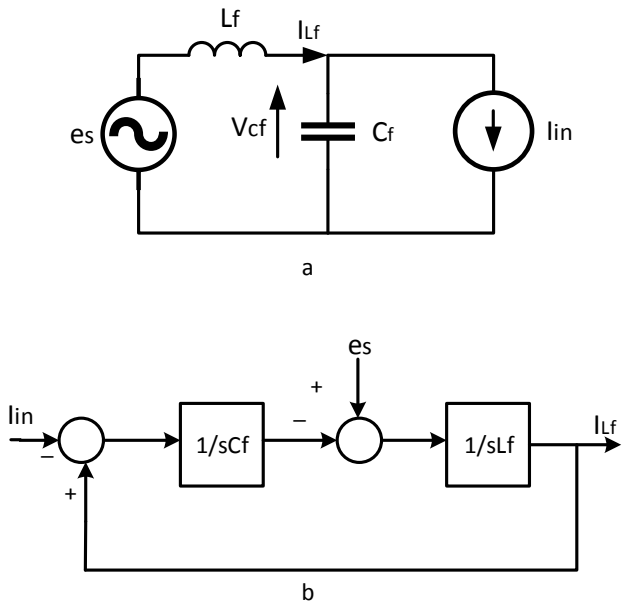

Fig. 3. a) Equivalent circuit of single-phase rectifier. b) block diagram equivalent to single phase rectifier [6].

filter must be very low. Although, a combination of a large LC filter with noise resistance may cause very slow oscillation and response problems [7].

3. THE CONCEPT OF VIRTUAL RESISTANCE

Fluctuations in the LC circuit can be attenuated by using a resistor connected to the LC circuit. All electrical engineers understand this concept. Although damping fluctuations using resistors is very effective, it cannot be used at high powers due to high resistance losses. Understanding the basic principles of oscillation damping in an LC circuit using a resistor is proposed as the basis of the concept of virtual resistance. Figure 3a shows a circuit equivalent to the single-phase AC side of an AC-DC PWM converter. The i_{in} current source is the main component of the AC-DC phase input current of the PWM converter, which is assumed to be the same as the reference input current used to control the converter. The source voltage of the phase is e_s. Figure 3b shows a block diagram that can be used to analyse the dynamic behaviour of a circuit in Figure 3a. Based on the block diagram in Figure 3b, the following transfer function is obtained:

$$\frac{I_s}{I_{in}} = \frac{1}{1+S^2 L_f C_f} \quad \textbf{(1)}$$

$I_s(s)$, $V_{cf}(s)$, and $V_{in}(s)$ are the Laplace transform of the source current, the capacitor voltage of the filter, and the input current of the converter, respectively. And s is the Laplace operator. Equation 1 shows the relationship between source current and rectifier input current. And displays the source stream behavior. In practice, the oscillation state is usually quenched by losses in the LC circuit. Fluctuations can be neutralized or damped by using a resistor attached to the LC filter. The resistor can be connected in series or in parallel to the inductor or filter capacitor. Figure 4 shows the four possible resistance connections in the LC filter.

Figures 5 to 8 show block diagrams showing the effect of resistance to damping fluctuations for each possible connection. As

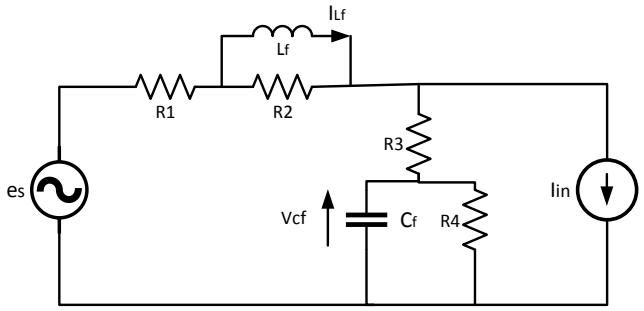

Fig. 4. Four possible resistor connections in the LC filter.

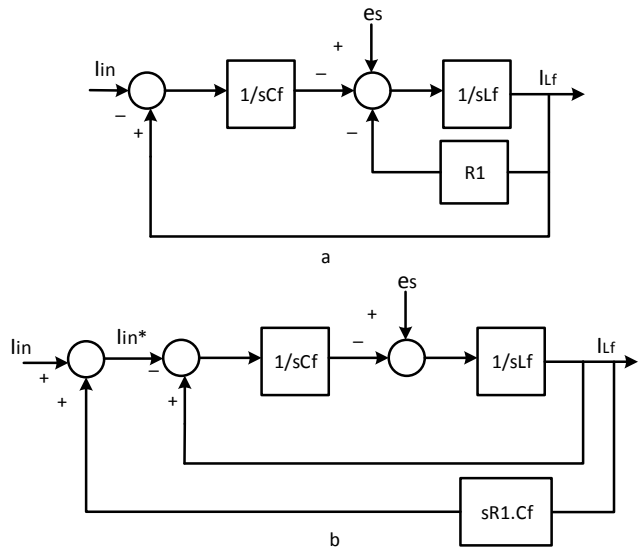

Fig. 5. a) The actual resistor R1 series with inductor. b) Manipulated diagram block of Figure a and represents the virtual resistance.

mentioned earlier, using a real resistor for oscillation damping significantly reduces system performance. If a virtual resistor that does not cause any losses replaces the real resistor, it can cause the damping to fluctuate without reducing efficiency. As shown by the block diagram in Figure 5a, the role of the series resistor with the inductor is to reduce the inductor voltage that is proportional to the current flowing through it. The block shape in Figure 5a can be shown in Figure 5b, which behave similarly. Because the block diagram in Figure 5b is the only result of manipulating the block in Figure 5a. Instead of using real resistors, Figure 5a shows the role of virtual resistors with a constant C1R1 coefficient in the inductor current derivative in Figure 5b. The output of the C1R1 derivative is injected into the i_{in} stream and collected. In a similar process, a virtual resistor equivalent to the real resistor can be created, as shown in Figures 6a, 7a, and 8a, which are equivalent to Figures 6b to 8b.

As shown in Figures 5 and 7, implementing a series virtual resistor with an inductor or filter capacitor requires a current sensor. According to Figures 6 and 8, a virtual resistor connected in parallel with the filter inductor or capacitor requires a voltage sensor and amplifier. Of the four virtual resistor connections, three connectors R1, R2 and R3 require the installation of a derivative. Because the jamming derivative may cause noise

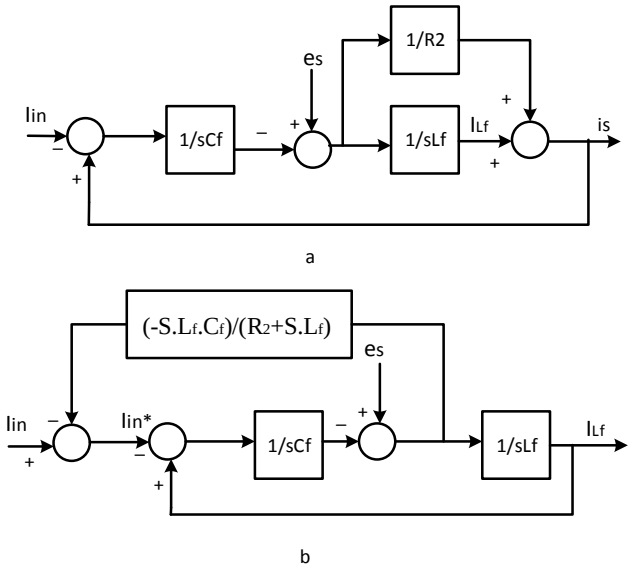

Fig. 6. a) The actual resistance R2 parallel to the inductor. b) Manipulated diagram block of Figure a and represents the virtual resistance.

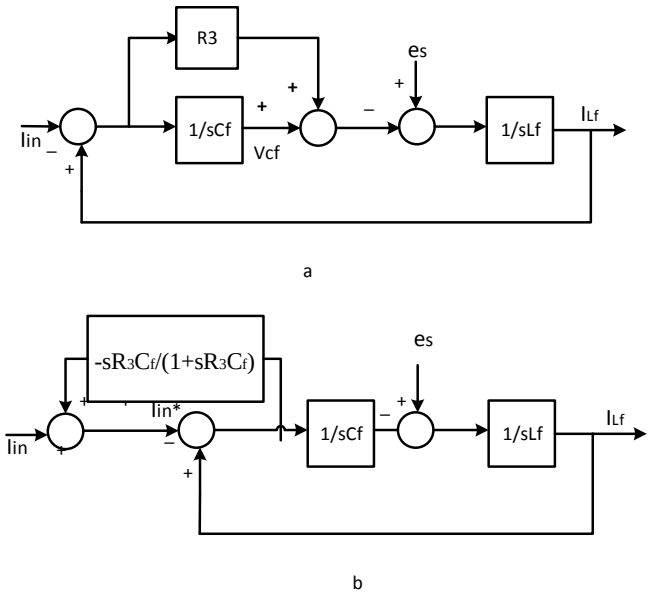

Fig. 7. a) The real resistance of R3 series with capacitor. b) Manipulated diagram block of Figure a and represents the virtual resistance.

problems and amplify high frequency signals. Only connecting a virtual resistor parallel to a capacitor does not require a derivative and is easier to implement. The application of the virtual resistance R4 can be seen in the block conversion function of Figure 8 shown in Equation 2.

$$\frac{I_s}{I_{in}} = \frac{1}{1+sL_f/R_4+s^2L_fC_f} \quad \textbf{(2)}$$

The addition of the sLf / R4 parameter to the denominator of Equation 2 indicates the effect of the virtual resistor on the charger. Compared to Equation 1, the denominator has changed.

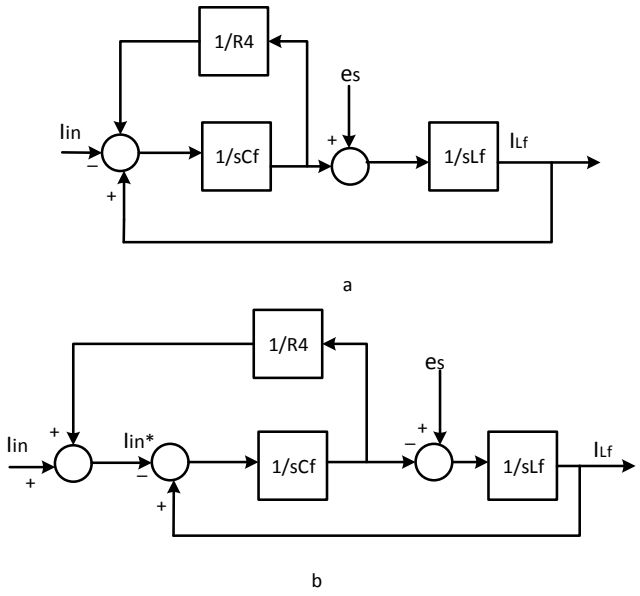

Fig. 8. a) The actual resistance R4 parallel to the capacitor. b) Manipulated diagram block of Figure a and represents the virtual resistance.

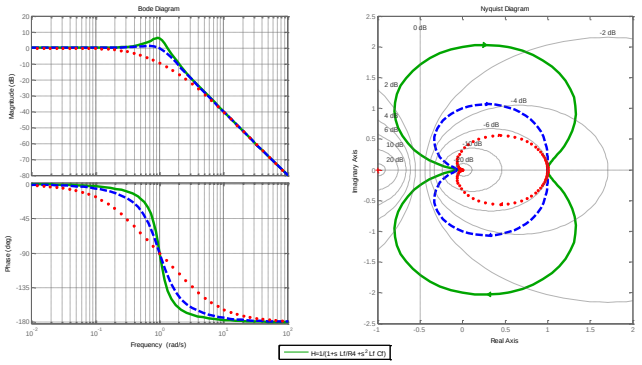

Fig. 9

4. CHECK THE PERFORMANCE OF THE SYSTEM IN EXCHANGE FOR THE APPLICATION OF VIRTUAL RESISTANCE USING GRAPHS AND NYQUIST

According to the relationships obtained in the previous section, it was a graph and Nyquist can be plotted and the system performance in terms of virtual resistance can be observed. For example, consider the equivalent circuit of Figure 8, in which resistor R4 is used in parallel with the filter capacitor. Figure 9a shows a diagram, and Figure 9b shows a Nyquist diagram in exchange for a change in resistor R4 in Equation 2 Which indicates an increase in system stability. This comparison can be seen similarly for other resistors.

5. SIMULATION RESULTS

To apply virtual resistance to the AC-DC controller, feedback from the capacitor voltage of the Vcf filter is required. The coefficient 1/R4 determines the amount of virtual resistance in the feedback. Figure 10 shows the proposed control block diagram for the application of virtual resistors. The PLL phase

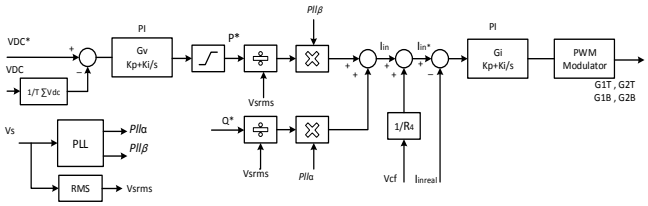

Fig. 10. Control diagram block with virtual resistance applied.

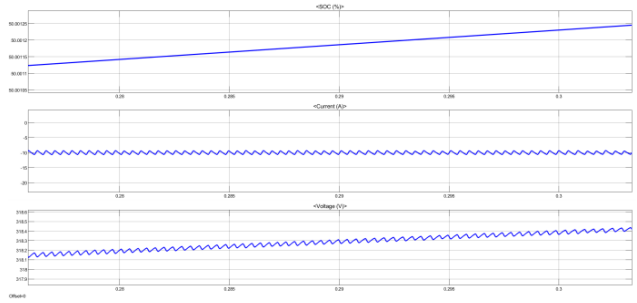

Fig. 11. View of changes in SOC, current and battery voltage in G2V mode.

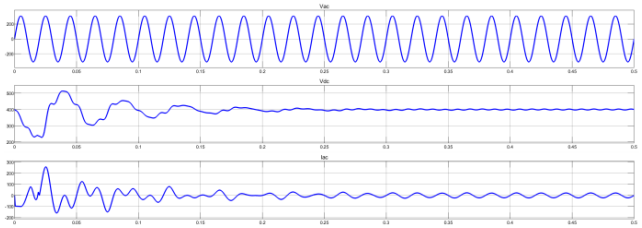

Fig. 12. View of the input current and voltage and the dc output voltage of the rectifier.

controller is also used in the control block. Reference Q^* indicates the amount of reactive power injected or absorbed by the rectifier. In G2V mode, the charger draws power from the network. Reference current is provided for the 10 amp battery charger. It should be noted that the amount of reactive power is considered zero. The initial charge of the battery is set at 50%. Changes in voltage, battery current, and SOC charging mode of the battery in network-to-vehicle mode are shown in Figure 11. Figure 12 shows the input current to the charger. The uniformity of voltage and current indicates the receipt of power with a unit of power from the network. Figure 13 shows the two controller modes without virtual resistor and with virtual resistor. With the application of THD virtual resistance feedback, the input current has been reduced from 6% to 3.6%.

6. LABORATORY IMPLEMENTATION

In this section, a virtual resistor parallel to a capacitor is used to implement the proposed method. In this test, capacitor, self-filter, control board and power board, as well as car battery were used. In this experiment, due to the lack of access to a large number of batteries and its high cost, a car battery was used to perform the test. The purpose of observing the performance of the new controller and also its effect is to reduce the input harmonic current.

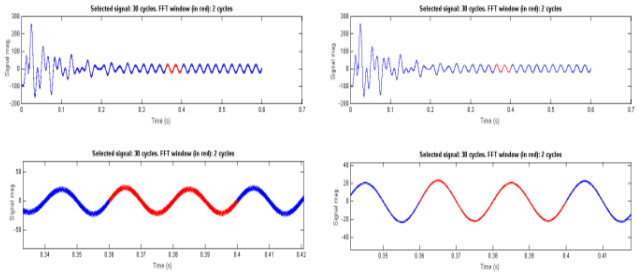

Fig. 13. Rectifier input flow diagram in two modes without virtual resistance and with virtual resistance.

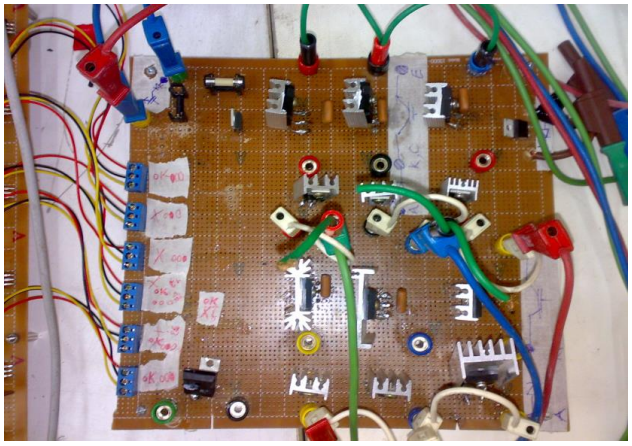

Fig. 14. Power circuit board.

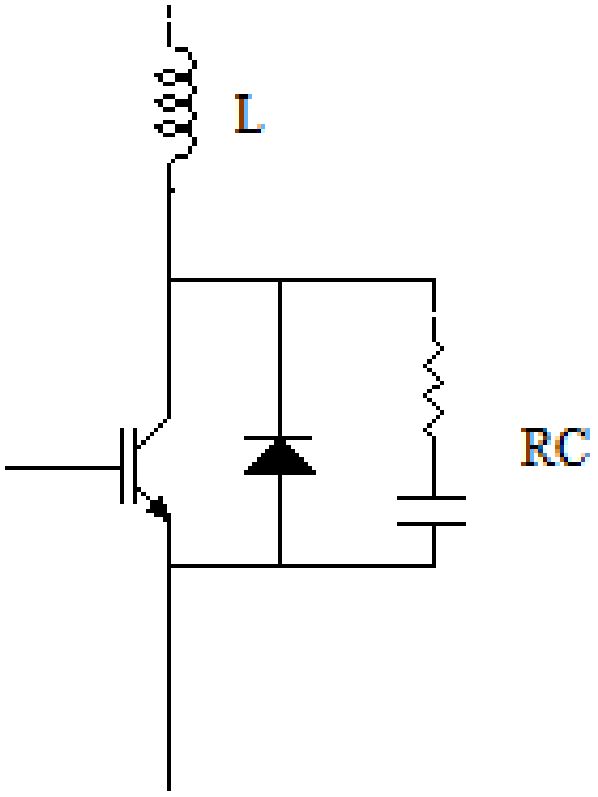

Fig. 15. Snubber circuit.

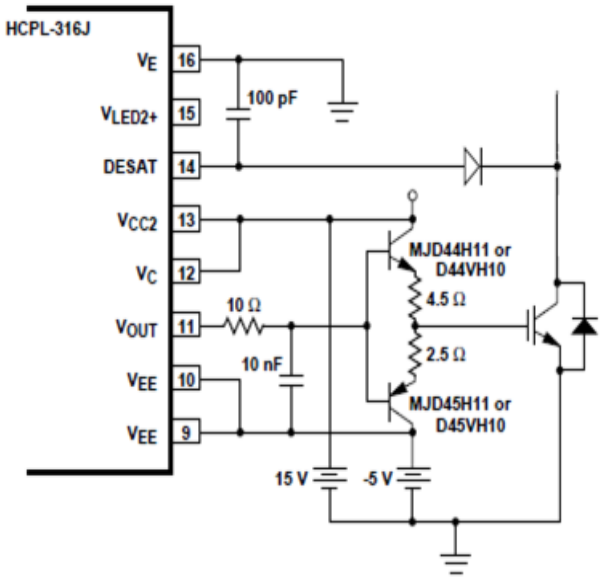

Fig. 16. HCPL chip output circuit with push-pull circuit.

A. Rectifier power board

Due to the limited access to the equipment, as well as the need for switches with suitable switching speed and high current, IGBT-Diode has been used in the construction of the power board among the power switches. The power board image is shown in Figure 14.

To limit $\frac{dv}{dt}$ a parallel RC shock absorber is usually used at both ends of the power semiconductor unit. L-series inductance is used to limit $\frac{di}{dt}$ as a series shock absorber. Figure 15 shows an example of a shock absorber circuit.

B. HCPL driver board

The introduced driver circuit includes a chip called HCPL316J, which is designed for IGBT power drivers. Features of this chip include the ability to drive with zero and one logic, error detection in case of problems in IGBT, the ability to reset the chip in the event of an error and a wide range of supply voltage from 15 to 30 volts. Push-pull circuitry has been used to increase the chip output current flow to the IGBT gate Which is shown in Figure 16.

C. Sudden changes in $\frac{dv}{dt}$ voltage and Miller current control

Due to the high switching speed of the power elements, sudden voltage changes of $\frac{dv}{dt}$ when the IGBT is turned off cause a current spike. The presence of a capacitor between the collector base and the IGBT gate (Miller capacitor) causes the current spike path (Miller current) to be transmitted to the gate through this capacitor. Miller current due to passing through the gate causes voltage spike on the base of the gate and losses. To prevent damage to the gate, the driver creates a path to drain the miller current using a gate resistor and a 47 KΩ esistor. To increase the speed of the miller discharge and reduce losses, the driver activates the 50x transistor when the switch is disconnected so

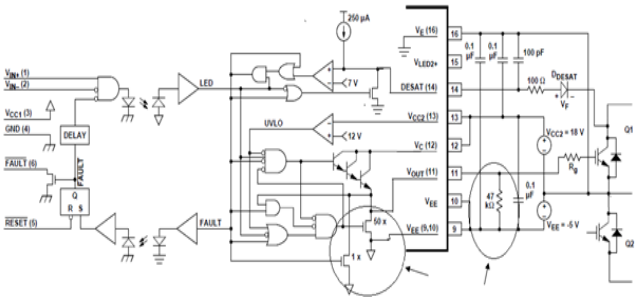

Fig. 17. Location of the 47 kh resistor and the 50x transistor (Miller clamp) [3].

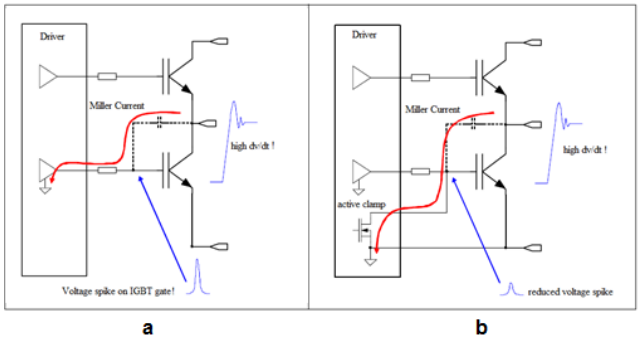

Fig. 18. Decreased gate voltage spike due to increased Miller current discharge rate a) Miller current discharge in driver resistance b) Rapid discharge of miller current with 50 x transistor inside driver.

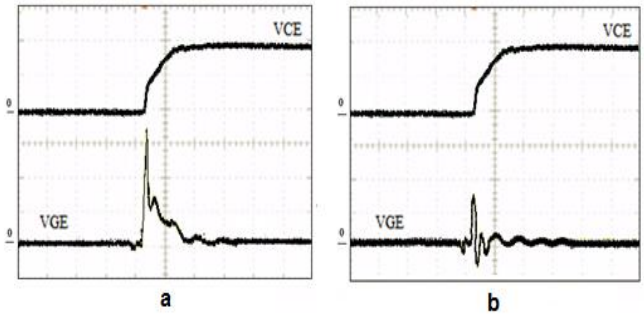

Fig. 19. Spike waveform of the voltage generated by the discharge of the Miller current a) Miller current discharge in driver resistance (gate voltage spike-emitter 3 volts) b) Rapid discharge of miller current with 50 x transistor inside the driver (gate voltage spike-emitter 1 volts)

that the miller current in the discharge path passes only through the gate resistor (Figures 17-19). In power drivers, applying reverse voltage at switch off time reduces off-time losses and improves $\frac{dv}{dt}$ transient mode. Increasing the output current of the chip by using an external buffer reduces switching losses [3].

Figure 20 shows how the chip works in the control system error mode. In case of an error in the control system, the reset option is used to fix the error instantly. The circuit used to drive the driver, including resetting the circuit and troubleshooting, is shown in Figure 21, using a global reset. If there is an error

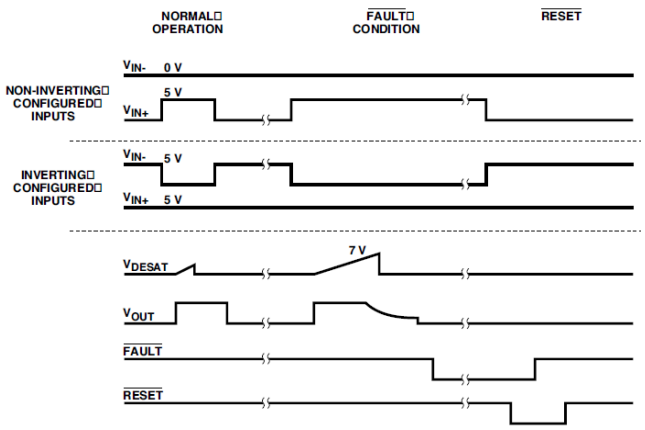

Fig. 20. Driver circuit operation in different conditions.

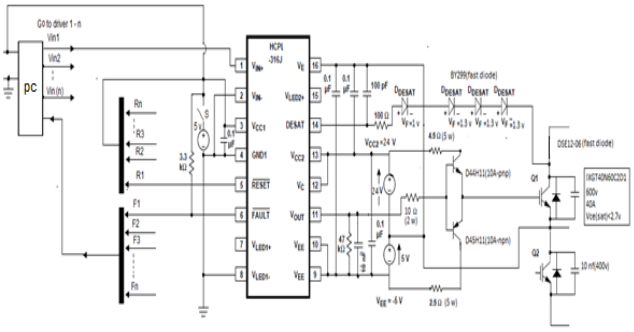

Fig. 21. Final and proposed circuit of the IGBT driver.

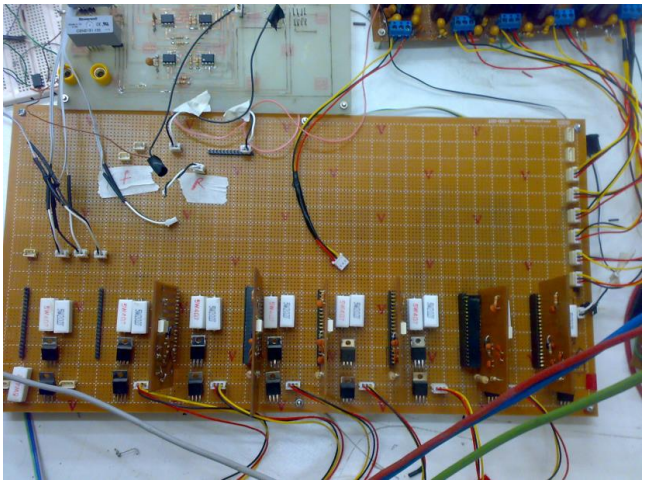

Fig. 22. HCPL driver board.

in the circuit, the entire control circuit is reset, and if the error is resolved, the system will continue to operate automatically. Figure 22 shows a view of the driver circuit consisting of the HCPL chip and peripherals.

D. Driver power supply

Due to the arrangement of IGBT power switches in the rectifier to power the power gate switch, the output side of the drivers can not be shared, because the negative end of the supply volt-

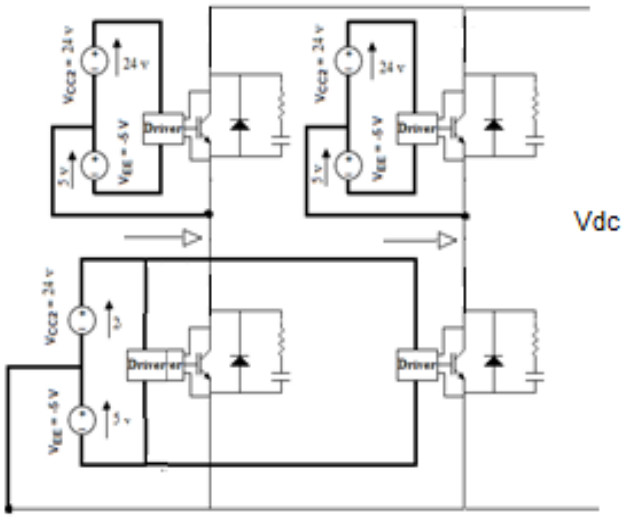

Fig. 23. How to connect the driver power supplies to the rectifier.

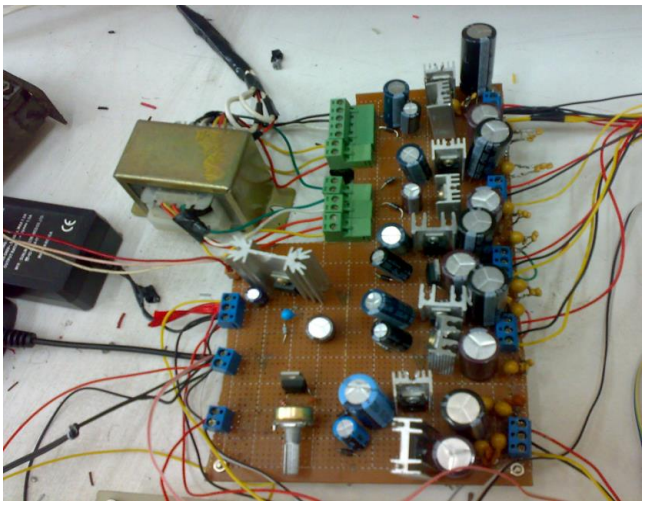

Fig. 24. Driver power supply circuit.

age in each driver is given to the IGBT emitter and if the power is shared between them two The input phases are short-circuited. Thus, three supply voltages of 24 and 5 volts are required, two of which are related to the three high switches and the other jointly to the two low switches. Figure 23 shows how to connect the driver power supplies. Isolated transformer with three separate outputs has been used to provide separate voltage sources. Figure 24 shows a view of the driver power supply circuit.

E. DSP processor

A DSP processor is used to process the data and send the command to the control board. High speed data processing capability and high accuracy are the features of this processor Shown in Figure 25.

F. Controller interface board

The control interface is used to transmit command signals from the processor to the driver, as well as to receive information from current sensors, as well as to amplify the command signals, as

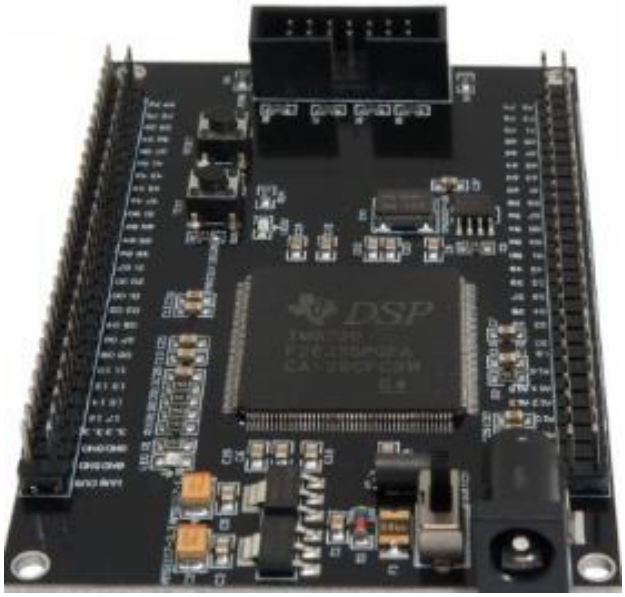

Fig. 25. DSP processor board.

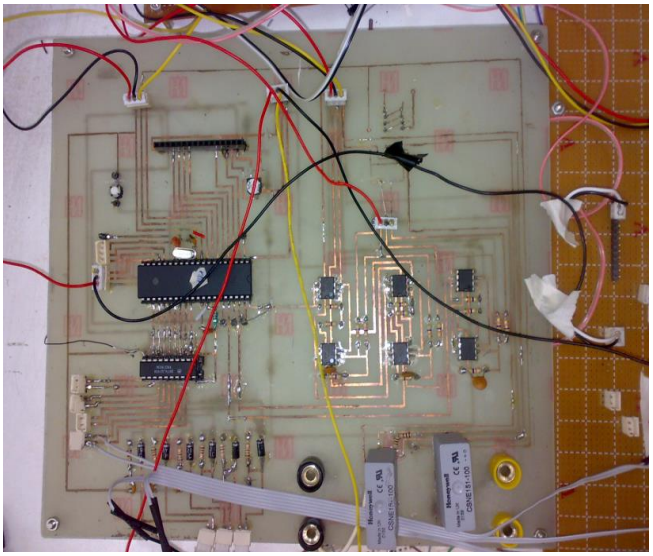

Fig. 26. Control interface board with buffer and current sensors.

shown in Figure 26. The use of a current sensor (CSNE151-100), in addition to proper accuracy, also separates the operation of the DSP logic circuits from the power supply. The sensor used in this dissertation is made by "honeywell" company, the specifications of which are given in Table 1. Since the current of the power circuit is not more than 3 amps, the arrangement of the last row of the table was used. As shown in Figure 27, the power supply of this sensor is symmetrical - 12 and 12 volt. Its output is flow type. To connect to the DSP, it must be converted to voltage by a grounded impedance. Depending on the resistance used, the output voltage will change, so the necessary normalization must be applied to the DSP processor program. Since digital processors do not have the ability to convert negative analog to digital values, a collector circuit has been used to solve this

Table 1. Specifications of the current sensor and how to connect the pins

primary turns	primary current nom, Ipn(A)	primary current max,Ip(A)	primary current max,Ip(A)	pin connection
1	25	44	25	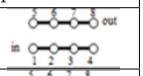
2	12	22	24	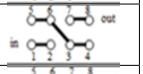
3	8	14	24	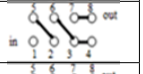
4	6	11	24	

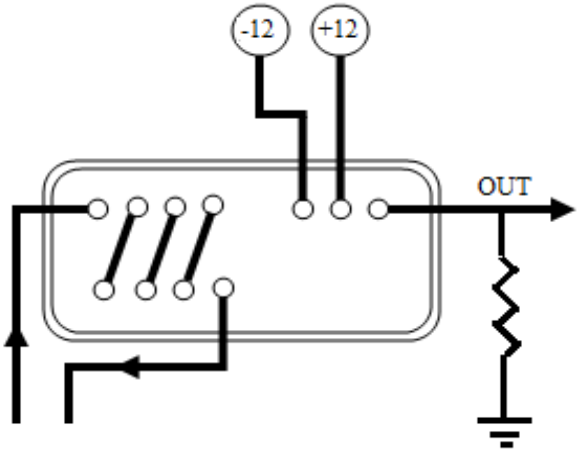

Fig. 27. How to connect the pins and power the current sensor.

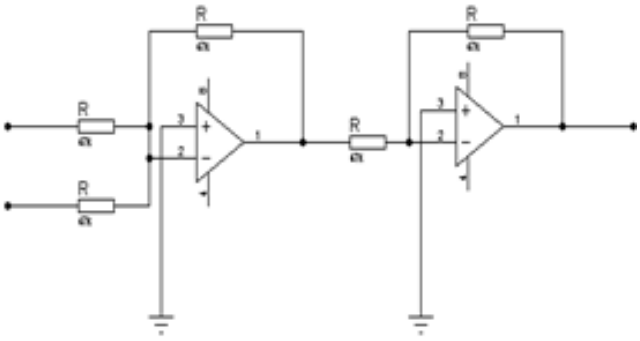

Fig. 28. Addition of dc voltage to current sensor output.

problem. According to the circuit of Figure 28, first a constant amount of DC is added to the motor current using an operational amplifier. Because the sum accumulated is inverted. Using another operational amplifier, correct the accumulated value so that the current is always positive. Within the program, a constant DC value is subtracted from the current value.

G. Inductor, capacitor and battery

According to Figure 29, the charger input inductor with a capacity of 100 mAh and a capacitor with a capacity of 1000 microfarads are located at the charger input. A 12-volt lithium-ion battery was used to test the control method. An overview of the control circuit and rectifier power is given in Figure 30. The

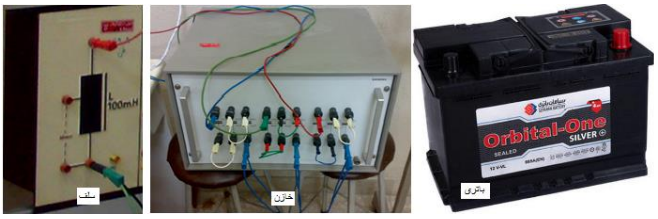

Fig. 29. Battery, capacitor and filter inductance in the charger.

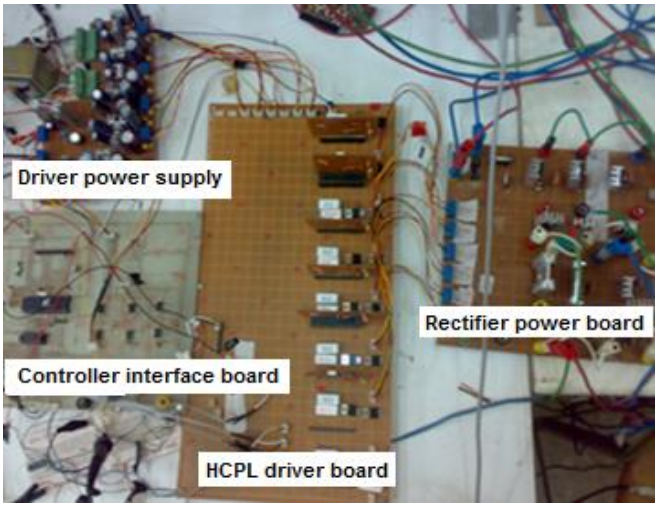

Fig. 30. Overview of the power circuit and charger controller.

reason for using separate sections is that these boards can be used for other experiments. For example, this board can be used as an inverter by changing its connections.

H. lab results

The ultimate goal of this test is to harmonically reduce the charger input current by applying virtual resistance feedback to the charger controller. Therefore, to show the correct performance of this control method, we need to display the charger input current in two modes without virtual resistance feedback and with virtual resistance feedback. Also, the DC voltage level of the battery, which is charging for 5 hours, is shown in Figure 31.

Figure 32 compares the Iac1 current and the Iac2 current. It is clear from the appearance of the diagram that the Iac2 current has less harmonic. And such an idea can be used at larger charger scales to reduce injected harmonics to the grid.

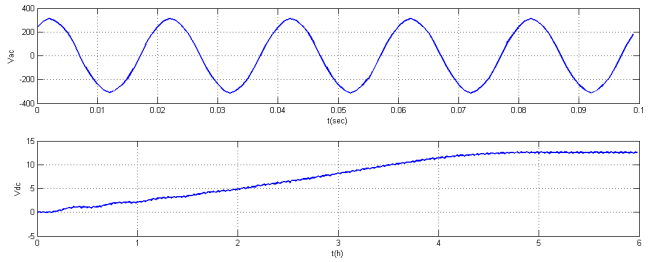

Fig. 31. Vac: Input voltage to the charger. Vdc: Battery voltage 12 volt.

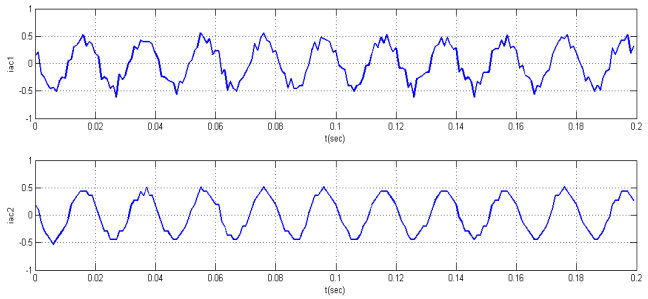

Fig. 32. Iac1: Charger input current without virtual resistor controller. Iac2: Charger input current with virtual resistor controller.

7. CONCLUSION

A new concept of virtual resistance is proposed in this paper to dampen fluctuations in the LC filter input of AC-DC PWM converters. Virtual resistors can counteract fluctuations without compromising the performance of converters. The virtual resistor can be connected in series or in parallel with the inductor or filter capacitor. It has been used in various papers about the use of virtual resistance to reduce transient oscillations.It is also used to dampen skips caused by keying and jumps caused by keying mistakes. And it is usually used in low powers.But the innovation of this paper is the reduction of network fluctuations in steady state caused by high power consumers. Especially, in charging stations that can be considered as the most common equipment in cities in the near future. And one of its advantages is the use of minimal equipment and without adding a new sensor to the control system, which can reduce costs. And also the elimination of the derivative in the new control circuit, which reduces the possibility of error in the implementation.The simulation results show the effectiveness of the proposed method. Expansion of the proposed concept for other applications and other converters is under consideration. And in the continuation of research, the effect of virtual resistance in reducing the output voltage of the rectifier output can be investigated.

REFERENCES

1. S. Haghbin, S. Lundmark, M. Alakula, O. Carlson,"Grid-connected integrated battery chargers in vehicle applications: Review and new solution". IEEE Transactions on Industrial Electronics. 2012 Feb 10;60(2):459-73.
2. M. Yilmaz, P.T. Krein,"Review of battery charger topologies, charging power levels, and infrastructure for plug-in electric and hybrid vehicles", IEEE transactions on Power Electronics. 2012 Aug 23;28(5):2151-69.
3. A. Khaligh, S. Dusmez,"Comprehensive topological analysis of conductive and inductive charging solutions for plug-in electric vehicles", IEEE Transactions on Vehicular Technology. 2012 Aug 13;61(8):3475-89.
4. SG. Jeong, WJ. Cha, SH. Lee, JM. Kwon, BH. Kwon. "Electrolytic capacitor-less single-power-conversion on-board charger with high efficiency". IEEE Transactions on Industrial Electronics. 2016 Jul 13;63(12):7488-97.
5. B.Whitaker, A. Barkley, Z. Cole, B. Passmore, D. Martin, TR. McNutt, AB. Lostetter, JS. Lee, K. Shiozaki, " A high-density, high-efficiency, isolated on-board vehicle battery charger utilizing silicon carbide power devices". IEEE Transactions on Power Electronics. 2013 Aug 28;29(5):2606-17.
6. Urtasun Erburu, A., Berrueta Irigoyen, A., Sanchis Gúrpide, P., Marroyo Palomo, L. (2018). Parameter-independent control for battery chargers based on virtual impedance emulation. IEEE Transactions on Power Electronics, vol. 33, no. 10, pp. 8848-8858, Oct. 2018.
7. Fu, Y., Li, Y., Huang, Y., Lu, X., Zou, K., Chen, C., Bai, H. (2018). Imbalanced load regulation based on virtual resistance of a three-phase four-wire inverter for EV vehicle-to-home applications. IEEE Transactions on Transportation Electrification, 5(1), 162-173.
8. Urtasun, A., Sanchis, P., Guinjoan, F., Marroyo, L. (2019). Parameter-independent battery control based on series and parallel impedance emulation. IEEE access, 7, 70021-70031.
9. T. Mishima, K. Akamatsu, M. Nakaoka, " A high frequency-link secondary-side phase-shifted full-range soft-switching PWM DC–DC converter with ZCS active rectifier for EV battery chargers". IEEE Transactions on Power Electronics. 2013 Apr 12;28(12):5758-73.
10. M. Kwon, S. Choi, " An electrolytic capacitorless bidirectional EV charger for V2G and V2H application". IEEE Transactions on Power Electronics. 2016 Nov 18;32(9):6792-9.
11. KM. Yoo, KD. Kim, JY. Lee, " Single-and three-phase PHEV onboard battery charger using small link capacitor". IEEE Transactions on Industrial Electronics. 2012 Jun 4;60(8):3136-44.
12. L. Wang, B. Zhang, D. Qiu, " A novel valley-fill single-stage boost-forward converter with optimized performance in universal-line range for dimmable LED lighting". IEEE Transactions on Industrial Electronics. 2016 Dec 6;64(4):2770-8.
13. Y. Wang, N. Qi, Y. Guan, C. Cecati, D. Xu, " A single-stage LED driver based on SEPIC and LLC circuits". IEEE Transactions on Industrial Electronics. 2016 Sep 27;64(7):5766-76.
14. G.Moschopoulos, P. Jain, " Single-phase single-stage power-factor-corrected converter topologies", IEEE Transactions on Industrial Electronics. 2005 Feb 7;52(1):23-35.
15. S. Li, J. Deng, CC. Mi, " Single-stage resonant battery charger with inherent power factor correction for electric vehicles". IEEE Transactions on Vehicular Technology. 2013 May 30;62(9):4336-44.
16. JY. Lee, YD. Yoon, JW. Kang, " A single-phase battery charger design for LEV based on DC-SRC with resonant valley-fill circuit", IEEE Transactions on Industrial Electronics. 2014 Aug 28;62(4):2195-205.
17. NQ. Trong, HJ. Chiu, YK. Lo, CY. Lin, MM. Alam, " Modified current-fed full-bridge isolated power factor correction converter with low-voltage stress", IET Power Electronics. 2013 Oct 30;7(4):861-7.
18. C. Li, Y. Zhang, Z. Cao, XU. Dewei, " Single-phase single-stage isolated ZCS current-fed full-bridge converter for high-power AC/DC applications". IEEE Transactions on Power Electronics. 2016 Nov 1;32(9):6800-12.
19. SW. Lee, HL. Do, " Single-stage bridgeless AC–DC PFC converter using a lossless passive snubber and valley switching". IEEE Transactions on Industrial Electronics. 2016 Jun 7;63(10):6055-63.
20. WY. Choi, " Single-stage battery charger without full-bridge diode rectifier for light electric vehicles". Electronics letters. 2011 May 12;47(10):617-8.
21. WY. Choi, JS. Yoo, " A bridgeless single-stage half-bridge AC/DC converter". IEEE Transactions on Power Electronics. 2011 Apr 7;26(12):3884-95.
22. DS. Gautam, F. Musavi, M. Edington, W. Eberle, WG. Dunford , " An automotive onboard 3.3-kW battery charger for PHEV application". IEEE Transactions on Vehicular Technology. 2012 Jul 25;61(8):3466-74.

23. PQ. Sinusoidal, "Non sinusoidal, Balanced or Unbalanced Conditions". IEEE Std. 1459-2000. 2009 May.
24. KY.Kim, SH. Park, SK. Lee SK, TK. Lee, CY. Won, " Battery charging system for PHEV and EV using single phase AC/DC PWM buck converter". IEEE Vehicle Power and Propulsion. Conference 2010 Sep 1 (pp. 1-6). IEEE.
25. M. Pahlevaninezhad, P. Das, J. Drobnik, PK. Jain, A. Bakhshai, " A new control approach based on the differential flatness theory for an AC/DC converter used in electric vehicles". IEEE Transactions on power electronics. 2011 Sep 29;27(4):2085-103.
26. L.Huber, Y. Jang, MM. Jovanovic," Performance evaluation of bridgeless PFC boost rectifiers". IEEE transactions on power electronics. 2008 May 2;23(3):1381-90.
27. R. Metidji, B. Metidji, B. Mendil , " Design and implementation of a unity power factor fuzzy battery charger using an ultrasparse matrix rectifier". IEEE transactions on power electronics. 2012 Aug 10;28(5):2269-76.
28. X. Zhou, G. Wang, S. Lukic, S. Bhattacharya, A. Huang, " Multi-function bi-directional battery charger for plug-in hybrid electric vehicle application". IEEE energy conversion Congress and exposition. 2009 Sep 20 (pp. 3930-3936). IEEE.
29. DC. Erb, OC. Onar, A. Khaligh, " Bi-directional charging topologies for plug-in hybrid electric vehicles. In2010 Twenty-Fifth Annual", IEEE Applied Power Electronics Conference and Exposition (APEC) 2010 Feb 21 (pp. 2066-2072).
30. V. Monteiro, H. Gonçalves, JC. Ferreira, Jl. Afonso, JP. Carmo, JE. Ribeiro, " Batteries charging systems for electric and plug-in hybrid electric vehicles". InNew Advances in Vehicular Technology and Automotive Engineering. 2012 Aug 1 (pp. 149-168). InTech.
31. OC. Onar, J. Kobayashi, DC. Erb, A. Khaligh, " A bidirectional high-power-quality grid interface with a novel bidirectional noninverted buck–boost converter for PHEVs". IEEE Transactions on Vehicular Technology. 2012 Apr 4;61(5):2018-32.
32. YJ. Lee, A. Khaligh, A. Emadi, " Advanced integrated bidirectional AC/DC and DC/DC converter for plug-in hybrid electric vehicles". IEEE Transactions on vehicular technology. 2009 Jul 21;58(8):3970-80.
33. SY. Kim, HS. Song, K. Nam," Idling port isolation control of three-port bidirectional converter for EVs". IEEE Transactions on Power Electronics. 2011 Oct 14;27(5):2495-506.
34. JG. Pinto, V. Monteiro, H. Gonçalves, JL. Afonso , " Onboard reconfigurable battery charger for electric vehicles with traction-to-auxiliary mode". IEEE Transactions on vehicular technology. 2013 Sep 25;63(3):1104-16.
35. GY. Choe, JS. Kim, BK. Lee, CY. Won, TW. Lee,"A Bi-directional battery charger for electric vehicles using photovoltaic PCS systems". In2010 IEEE Vehicle Power and Propulsion Conference. 2010 Sep 1 (pp. 1-6). IEEE.
36. PA. Dahono," A control method to damp oscillation in the input LC filter". IEEE 33rd Annual IEEE Power Electronics Specialists Conference. Proceedings (Cat. No. 02CH37289) 2002 Jun 23 (Vol. 4, pp. 1630-1635). IEEE.
37. PA. Dahono, YR. Bahar, Y. Sato, T. Kataoka, " Damping of transient oscillations on the output LC filter of PWM inverters by using a virtual resistor". In4th IEEE International Conference on Power Electronics and Drive Systems. IEEE PEDS 2001-Indonesia. Proceedings (Cat. No. 01TH8594) 2001 Oct 25 (Vol. 1, pp. 403-407). IEEE.
38. AK. Adapa , V. John, "Virtual resistor based active damping of LC filter in standalone voltage source inverter".In2018 IEEE Applied Power Electronics Conference and Exposition (APEC) 2018 Mar 4 (pp. 1834-1840). IEEE.
39. DS. Gautam, F. Musavi, M. Edington, W.Eberle, WG. Dunford, " An automotive onboard 3.3-kW battery charger for PHEV application". IEEE Transactions on Vehicular Technology. 2012 Jul 25;61(8):3466-74.
40. S. Kim, FS. Kang, " Multifunctional onboard battery charger for plug-in electric vehicles". IEEE Transactions on Industrial Electronics. 2014 Dec 4;62(6):3460-72.
41. K. Yao, Y. Wang, J. Guo, K. Chen, " Critical conduction mode boost PFC converter with fixed switching frequency contro". IEEE Transactions on Power Electronics. 2017 Sep 29;33(8):6845-57.